HHS Public Access

Author manuscript

ACS Appl Mater Interfaces. Author manuscript; available in PMC 2023 March 09.

Published in final edited form as:

ACS Appl Mater Interfaces. 2018 December 12; 10(49): 41892–41901. doi:10.1021/acsami.8b08920.

Tunable Hydrogels Derived from Genetically Engineered Extracellular Matrix Accelerate Diabetic Wound Healing

Aaron H. Morris[†,§], **Hudson Lee**[§], **Hao Xing**[†,§], **Danielle K. Stamer**[†], **Marina Tan**[†], **Themis R. Kyriakides**[*,†,‡,§]

[†]Department of Biomedical Engineering, Yale University, New Haven, Connecticut 06511, United States

[‡]Department of Pathology, Yale University, New Haven, Connecticut 06511, United States

[§]Vascular Biology and Therapeutics Program, Yale University, New Haven, Connecticut 06511, United States

Abstract

Hydrogels composed of solubilized decellularized extracellular matrix (ECM) are attractive materials because they combine the complexity of native ECM with injectability and ease of use. Nevertheless, these materials are typically only tunable by altering the concentration, which alters the ligand landscape, or by incorporating synthetic components, which can result in an unfavorable host response. Herein, we demonstrate the fabrication of genetically tunable ECM-derived materials, by utilizing wild type (WT) and (thrombospondin-2 knockout) TSP-2 KO decellularized skins to prepare hydrogels. The resulting materials exhibited distinct mechanical properties characterized by rheology and different concentrations of collagens when characterized by quantitative proteomics. Mixtures of the gels achieved intermediate effects between the WT and the KO, permitting tunability of the gel properties. In vivo, the hydrogels exhibited tunable cell invasion with a correlation between the content of TSP-2 KO hydrogel and the extent of cell invasion. Additionally, TSP-2 KO hydrogels significantly improved diabetic wound healing at 10 and 21 days. Furthermore, hydrogels derived from genetically engineered in vitro cell-derived matrix mimicked the trends observed for tissue-derived matrix, providing a platform for faster screening of novel manipulations and easier clinical translation. Overall, we demonstrate that genetic engineering approaches impart tunability to ECM-based hydrogels and can result in materials capable of enhanced regeneration.

Graphical Abstract

[*]**Corresponding Author**: themis.kyriakides@yale.edu. 10 Amistad St. Room 301C, New Haven, CT 06519, United States.

Author Contributions

This work is part of the Ph.D. thesis of A.H.M. guided by T.R.K. A.H.M., H.L., D.K.S., H.X., and M.T. conducted experiments and analyzed data. A.H.M and T.R.K. designed experiments, and A.H.M. wrote the manuscript. All authors provided input on the manuscript and have approved the final version.

Supporting Information

The Supporting Information is available free of charge on the ACS Publications website at DOI: 10.1021/acsami.8b08920.

Rheology of tissue-derived hydrogels at 4 and 6 mg/mL, diffusion through hydrogels, in vitro fibroblast migration into hydrogels, and SDS–PAGE of pre-gel solutions (PDF)

Proteomics data for all unique proteins detected (Table S1) (XLSX)

The authors declare no competing financial interest.

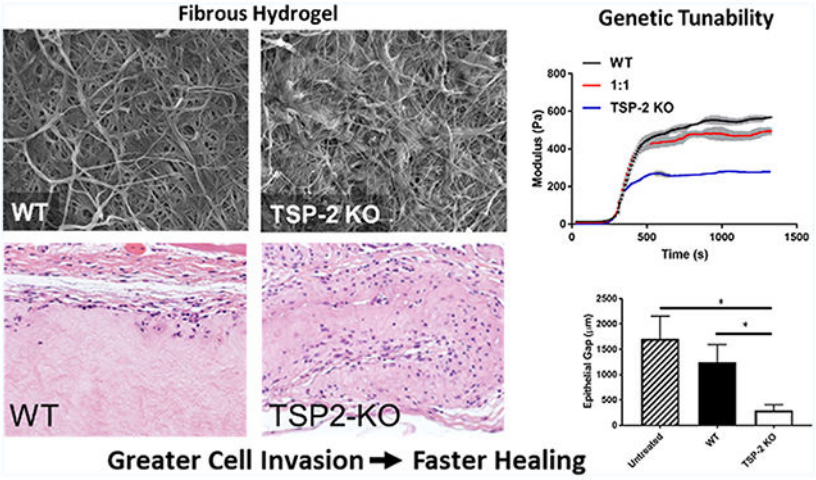

Keywords

hydrogel; ECM (extracellular matrix); wound healing; regenerative medicine; tissue engineering; genetically modified matrix

INTRODUCTION

Regenerative medicine approaches seek to enable the reconstruction of damaged tissues through drug delivery, cell therapy, or scaffold-mediated repair.[1] Hydrogels, composed of synthetic or natural polymers swollen with water, have become an attractive class of materials implemented in regenerative medicine strategies because they are capable of eluting drugs, retaining cells at a site of delivery, and serving as a reconstructive scaffold.[2–5] Hydrogels capable of in situ gelation in a host are being investigated with increasing frequency because they can be deployed through minimally invasive techniques (such as simple injection) and can rapidly fill void spaces of complex geometries.

To date, most hydrogels investigated are synthetic in origin because of their enhanced tunability and ease of manufacturing. Nevertheless, there has been a recent push toward hydrogels of naturally derived origin because of their distinct advantages over synthetics.[6–9] Moreover, significant work has investigated hydrogels derived from decellularized extracellular matrix (ECM), because ECM-derived materials have a number of advantages, including matrix-bound growth factors, endogenous degradation pathways, and a favorable host response.[9–11] These materials are most commonly prepared by solubilizing decellularized ECM-based materials in an acidic pepsin solution; buffering of the solution then permits temperature-sensitive polymerization via self-assembly of collagen monomers. Because their composition is similar to that of decellularized tissues, the regenerative benefits of decellularized tissues are retained with ECM-derived hydrogels and may even be enhanced due to partial degradation of the material.[9,11–14] Indeed, the host response to ECM-based hydrogels is similar to that to decellularized tissues with early interrogation by neutrophils and macrophages and subsequent invasion by stem cells and migratory cells from the surrounding tissue.[4,15] Furthermore, it has been demonstrated

that ECM-based hydrogels can promote angiogenesis, an ideal effect in the context of regenerative medicine.[12]

Another advantage that ECM hydrogels have over bulk decellularized materials is that investigators can more easily manipulate the properties of hydrogels than intact decellularized tissues. Because tissue-derived hydrogels are liquid before gelation, it is easy to envision adding molecules or cells simply by mixing, imparting more engineering control.[16–18] Recent studies have demonstrated that growth factors can easily be added to ECM-derived hydrogels, providing long-term growth factor release.[19,20] Additionally, changing the concentration of the ECM alters gel stiffness and the speed at which cells invade, at least in vitro.[21–24] Nevertheless, reducing gel concentration to change the mechanical properties will correspondingly reduce concentrations of various biochemical components and alter the ligand landscape within the gels, which may limit the regenerative potential of the gel.

Recent proof-of-concept work has demonstrated that genetic manipulations can impart some bottom-up control to decellularized materials.[25–28] Of particular interest is that acellular dermis derived from thrombospondin-2 (TSP-2) knockout (KO) animals exhibits an altered structure and mechanics compared to that from WT.[25] Because of these findings, we sought to engineer hydrogels from decellularized TSP-2 KO skin with beneficial properties not shared by hydrogels derived from WT. Additionally, because gels can be easily mixed, we combined WT and KO gels to construct the first tunable ECM materials (while maintaining a constant ECM concentration), which enables a far greater tunability than the binary approach achieved with intact acellular dermis. Moreover, this can be further extended to hydrogels constructed from cell-derived matrix (CDM), permitting further tunability and an easier path to clinical translation. Here, we show that these genetically tunable ECM materials exhibit altered material properties manifesting in tunable cell invasion and ultimately improved wound healing in vivo.

MATERIALS AND METHODS

Isolation and Decellularization of Murine Skin.

All procedures involving animal use were approved by the Animal Care and Use Committee of Yale University and abided by the regulations adopted by the National Institutes of Health. Murine skin was isolated and decellularized according to established protocols.[25,29]

Cell Culture.

Cells were maintained in vitro with standard protocols. Briefly, the mouse embryonic fibroblast cell line NIH/3T3 (ATCC) and mouse preosteoblastic cell line MC3T3-E1 were cultured in their respective growth media, DMEM and MEMα, supplemented with 10% FBS and 1% pen/strep.

Hydrogel Preparation.

ECM was solubilized by incubating decellularized WT or KO skin at 10 mg dry weight per milliliter of fluid in a solution of 1 mg/mL pepsin in 0.01 N HCl (Sigma) for 72

h as described previously.[25,30] The solubilized ECM was neutralized and buffered with sodium hydroxide (1/10 digest volume) and 10× phosphate-buffered saline (PBS) (1/9 digest volume). To prepare tissue-derived hydrogels, buffered and solubilized ECM was diluted to a final concentration of 8 mg/mL with PBS to form the pre-gel solution and stored on ice until use. WT/KO gels (1:1 ratio) were also prepared by mixing this solution of tissue-derived hydrogel in equal volumes. For the preparation of hydrogels from CDM, MC3T3-E1 cells were cultured at confluence in the presence of 100 μM ascorbic acid and 4 μM inositol hexakisphosphate (IP6; to prevent matrix mineralization) for 10 days.[31] Cells were decellularized with 40 mM NH_4OH and 0.5% Triton X-100 for 1 min and washed extensively with PBS. The ECM was rinsed with deionized water, scraped with a cell scraper into scintillation vials, and lyophilized. Hydrogels were prepared by incubating ECM at a concentration of 10 mg dry weight per milliliter of fluid in a solution of 1 mg/mL pepsin in 0.01 N HCl (Sigma) for 24 h before neutralization and buffering as described above.

Subcutaneous Injection.

All procedures involving animal use were approved by the Animal Care and Use Committee of Yale University and abided by the regulations adopted by the National Institutes of Health. Subcutaneous injection of tissue-derived hydrogels was performed by injecting 250 μL of pre-gel solution (kept on ice) subcutaneously for 5 days in 12–14 week old C57BL/6 mice. Each mouse received two injections in its dorsal region, each from a different genotype of gel (WT, KO, or 1:1). Implants were excised with the surrounding tissue intact, fixed in Z-fix (Anatech), and embedded in paraffin for sectioning. Sections were stained with hematoxylin and eosin (H&E) according to standard protocols, as well as for vimentin immunohistochemically (EMD Millipore). For analysis of cell penetration, three 20× images were taken per injection, and the average number of cells per high-power field was quantified ($n = 8$).

In Vivo Wound Healing in Diabetic Animals.

All procedures involving animal use were approved by the Animal Care and Use Committee of Yale University and abided by the regulations adopted by the National Institutes of Health. Twelve week old diabetic db/db mice (B6.BKS(D)-Leprdb/J, The Jackson Laboratory) were used for wound experiments as previously described.[25,32,33] Anesthesia was induced with isoflurane, and two full-thickness wounds were created on the dorsal region using a 6 mm biopsy (Acu-Punch). Wounds were covered with 40 μL of pre-gel solution, which filled the wound and gelled in situ, and the entire area was then covered with Tegaderm (3M), which was secured in place by sutures.

At 10 or 21 days, animals were euthanized and the wound area was excised and prepared for analysis as described above. Sections were stained with H&E according to standard protocols. For quantification of hydrogel-treated wounds, 10× images were stitched to cover the entire wound width. Wound width and epithelial gap were measured using ImageJ. Epithelial thickness and unremodeled gel thickness were determined by measuring at five locations throughout each wound. Additionally, samples were analyzed via immunohistochemistry with anti-CD31 (Dianova) and anti-αSMA (Dako) antibodies. For

quantifying cellular content of hydrogels after implantation in wounds, ImageJ was used to quantify the number of vimentin+ cells and the number and size of CD31+ and SMA+ lumens. Three 20× images were quantified per implant.

Gene Delivery to MC3T3-E1 Cells.

To create a stable cell line with reduced TSP-2 expression, a plasmid encoding a TSP-2 shRNA or its vector control (pSHAG-MAGIC vector) was transfected into MC3T3-E1 cells with Lipofectamine. Cells were then selected in puromycin (20 μg/mL, Thermo Fisher) to create a stable cell line. Reduction in TSP-2 expression was confirmed via Western blotting.

Turbidimetric Gelation Kinetics.

Hydrogel gelation kinetics was measured as previously described.[21] Briefly, 100 μL of neutralized pre-gel solution at a concentration of 4 mg/mL was loaded into 96-well plates on ice. Plates were then placed in a plate reader that was preheated to 37 °C, and gelation was tracked spectrophotometrically at 415 nm. Experiments were conducted at 4 mg/mL because, at higher concentrations, the solution was too turbid at time $t = 0$ to obtain accurate measurements. Readings were normalized with the following equation:[21]

$$\text{normalized absorbance} = \frac{A - A_0}{A_{\max} - A_0} \tag{1}$$

where A_0 is the initial absorbance, $A_{\max}$ is the maximum absorbance, and A is the given absorbance measurement.

Additionally, $t_{1/2}$ was calculated as the time to reach 50% absorbance ($n = 5$).

Scanning Electron Microscopy.

To prepare hydrogel samples for SEM, 250 μL of pre-gel solution was added to cloning rings and allowed to gel at 37 °C for 1 h. Hydrogel samples were then fixed in 2.5% paraformaldehyde in 0.1 M cacodylate buffer (Electron Microscopy Sciences), dehydrated with an ethanol gradient, incubated in hexamethyldisilazane (Electron Microscopy Sciences), and air-dried. All samples were sputter-coated with iridium and viewed by SEM (Hitachi SU-70).

Rheology.

Rheology was performed using an AR2000 rheometer (TA Instruments) with a 25 mm parallel plate geometry. Gap height was set to 700 μm (350 μm for CDM). The ECM pre-gel was pipetted onto the rheometer plate, which was maintained at a temperature of 10 °C using a Peltier temperature controller. Mineral oil was added to the edge to reduce evaporation of the samples. Temperature was increased stepwise by 1° and allowed to stabilize for 15 s before a measurement was taken. This procedure was followed until the temperature reached 37 °C, at which point the temperature was maintained to induce gelation. A frequency of 1 Hz and 3% strain were used to conduct measurements.

SDS–PAGE.

The ECM pre-gel was analyzed by SDS–PAGE on a 10% Tris-HCl polyacrylamide gel (Bio-Rad). Fifty micrograms of solubilized ECM was added to each lane and compared against the Precision Plus Protein Dual Color Ladder (Bio-Rad). Gels were stained with Coomassie blue and imaged with a LICOR infrared scanner.

Proteomics.

The buffered pre-gel was precipitated with chloroform–methanol–water and dried. Samples were digested with Lys-C and trypsin and subsequently prepared and analyzed as previously described by the Keck Foundation Biotechnology Resource Laboratory at Yale University.[34]

Statistical Analysis.

Data are expressed as mean + standard error of the mean (SEM). All statistical analyses of data with more than two samples were conducted using one-way ANOVA with Tukey's multiple comparison test. For analysis of cell penetration into WT, 1:1, and TSP-2 KO hydrogels at various depths, a two-way ANOVA with Tukey's multiple comparison test was used. For experiments where data were collected from only two samples, a two-tailed Student's *t* test was used. Values of $p < 0.05$ were considered statistically significant.

RESULTS

Genetic Manipulation Imparts Tunability to Material Properties of Tissue-Derived Hydrogels.

Tissue-derived hydrogels were prepared from decellularized WT and TSP-2 KO mouse skin by pepsin solubilization followed by neutralization and warming to 37 °C (Figure 1A). WT, TSP-2 KO, and a 1:1 mixture formed intact hydrogels with fibrillar structures (Figure 1D–F). Turbidimetric determination of gelation kinetics indicated the expected sigmoidal gelation curve regardless of genotype (Figure 1B). Interestingly, KO gels gelled slower than WT, and a 1:1 mixture had intermediate gelation times (Figure 1C). Rheology demonstrated a clear distinction in mechanical properties between the WT and TSP-2 KO gels. Specifically, they exhibited similar kinetics of gel stiffening, but the TSP-2 KO gel had a reduced storage modulus as compared to WT (Figure 1G,H). Additionally, a 1:1 mixture of WT and TSP-2 KO gel demonstrated a storage modulus that was reduced compared to WT but increased compared to TSP-2 KO, demonstrating that genetic modification of source tissue can yield a tunable tissue-derived hydrogel system through simple mixing (Figure 1G,H). Additionally, gels with lower ECM concentrations exhibited similar trends, with WT having the largest storage modulus and TSP-2 KO having the smallest storage modulus (Supporting Information Figure S1). Furthermore, there was no significant change in the rate at which molecules of various sizes (from small molecules through large proteins) diffuse through these materials, suggesting that they may provide a drug delivery system with tunable mechanics but consistent drug delivery profiles (Supporting Information Figure S2).

Protein Content.

Because WT and TSP-2 KO hydrogels displayed altered mechanical properties, analysis of protein content was an important consideration. SDS–PAGE analysis indicated that the gels were composed largely of collagen but that the TSP-2 KO gel exhibited qualitatively less collagen than WT (Figure 2A). This is consistent with previous findings that TSP-2 KO decellularized skin exhibits reduced collagen content compared to WT.[25] Proteomic analysis demonstrated significant differences in 11 proteins between WT and TSP-2 KO gels, most of which were collagens (Figure 2B,C). The $\alpha 4$ chain of collagen type 4 and the $\alpha 1$ chain of collagen type 6 were both increased in the TSP-2 KO gels, but various other collagens were contained at higher levels within the WT (Figure 2C).

Subcutaneous Injections of Hydrogel Indicate Tunable Host Response.

To assess tunability of the host response by genetic manipulation, hydrogels were injected subcutaneously into healthy mice and retrieved 5 days later. H&E staining of hydrogel sections showed that there was increased cell penetration into TSP-2 KO gels compared to WT (Figure 3A). There were significantly more cells able to invade the 1:1 WT/KO gel than the WT and significantly more in the TSP-2 KO gel than in the 1:1 mixture. Furthermore, the TSP-2 KO and 1:1 hydrogels promoted increased cell migration into the depth of the gel (Figure 3C). Immunohistochemical detection of vimentin indicated the presence of cells of mesenchymal lineage (Figure 3B). These findings mimic the in vitro observation that NIH/3T3 fibroblasts penetrated further into TSP-2 KO hydrogels than into WT (Supporting Information Figure S3) and suggest that through genetic manipulation of TSP-2, it is possible to tune an aspect of the host response to a hydrogel, namely, cell invasion.

Genetically Engineered Hydrogels Promote Diabetic Wound Healing.

To assess whether tunable hydrogels would demonstrate utility in a regenerative medicine setting, they were applied to full-thickness wounds in diabetic db/db mice for 10 and 21 days (Figures 4 and 5, respectively). By 10 days, the wounds had begun to heal and epithelialization was visible over the tissue-derived hydrogels; additionally, qualitatively more cells penetrated into the TSP-2 KO gels (Figure 4A). Wounds treated with TSP-2 KO gel demonstrated a smaller epithelial gap than untreated wounds or WT gel, suggesting improved healing (Figure 4B). Furthermore, TSP-2 KO gel displayed decreased thickness by 10 days, suggesting increased remodeling (Figure 4C). TSP-2 KO gel promoted vascularization of the surrounding wound bed by 10 days, demonstrating increased CD31+ lumen presence, size, and stabilization by smooth muscle cells (Figure 4D–H). By 21 days, all wounds had closed (Figure 5A–C), but TSP-2 KO hydrogel-treated wounds demonstrated decreased epithelial thickness (an indicator of maturity of a healed wound) compared to untreated control (Figure 5D). Additionally, the width of the wound bed was reduced in wounds treated with TSP-2 KO gel (Figure 5E). Overall, treatment of diabetic wounds with TSP-2 KO hydrogels demonstrated improved wound healing associated with improved epithelialization, gel remodeling, vascularization, and ultimately, a reduction in the overall size of the wound bed.

Genetic Manipulation Imparts Tunability to CDM Hydrogels.

Genetically tunable tissue-derived hydrogels establish a method of providing bottom-up tunability to ECM-based materials that can control material properties and enhance their regenerative potential. However, screening various genetic manipulations for advantageous benefit requires genetically engineered animals, and clinical translation likely requires creation of genetically engineered large animals. CDM has provided an alternative to tissue-derived ECM in applications where enhanced customizability (such as alterations in source species of ECM or mechanical conditioning) is desired.[35] CDM can be produced by cells from a desired species (including human) in a number of culture conditions and can even be genetically modified to include exogenous factors.[26] Because CDM serves as an ECM source beyond decellularized tissues, we hypothesized that hydrogels derived from CDM would provide an opportunity to overcome the obstacles associated with the discovery of novel genetic manipulations and translation of tissue-derived hydrogels. MC3T3-E1 pre-osteoblasts were chosen to construct CDM hydrogels because they produce a robust collagenous ECM in vitro. TSP-2 expression of MC3T3-E1 was knocked down via transfection with an anti-TSP-2 shRNA in a pSHAG-MAGIC vector (or vector control) as described previously.[36] Stable cell lines were created via selection in puromycin and TSP-2 knockdown (KD) was confirmed via Western blotting (Figure 6A). A Western blot for collagen indicated similar findings to tissue-derived hydrogels, demonstrating that the TSP-2 KD gel exhibited qualitatively less collagen than the vector control (Figure 6B). SDS–PAGE was also used to demonstrate similar overall protein makeup of the gels, with the gels consisting largely of collagen (Supporting Information Figure S4). Rheologically, CDM gels exhibited similar trends to their corresponding tissue-derived hydrogels, with the TSP-2 KD gel having a reduced storage modulus as compared to the pSHAG control (Figure 6C,D). Although the CDM gels had lower overall storage moduli than the tissue-derived gels, they exhibited a similar genetic tunability. We hypothesize that alterations in cell type, culture time, and CDM concentration will result in tunable ECM materials with several desirable properties.

DISCUSSION

A major limitation of decellularized materials is that engineering control of these materials is typically limited to top-down approaches such as adding exogenous growth factors, perforating the material, and blending synthetic and decellularized materials into biohybrid constructs.[37–45] Our laboratory has recently demonstrated proof-of-concept work that decellularized materials derived from genetic knockouts can be functionally distinct from materials derived from WT animals.[25] Nevertheless, tunable materials require a broader range than the simple binary selection that WT or KO implies. To construct genetically tunable ECM-derived materials, we turned to tissue-derived hydrogels created from decellularized WT and TSP-2 KO mouse skin. WT and TSP-2 KO gels displayed significantly different mechanical properties by rheology, and importantly, a 1:1 ratio of WT to TSP-2 KO hydrogel, prepared simply by mixing the two in equal parts, had intermediate mechanical properties. This result suggests that genetic manipulation of source animal tissue enables the creation of mechanically tunable hydrogels without adjusting the ECM concentration or incorporating any synthetic components, which is advantageous because

it allows adjustment of mechanical properties without altering the ligand concentration (as would be expected in gels tuned via concentration) and preserves the favorable host response to naturally derived materials by avoiding synthetic components. Genetically engineered materials should eventually enable selective enrichment and removal of components within a material, a particularly valuable approach for components for which there is no specific enzymatic degradation (such as TSP-2).

This work explores alterations in protein content of the hydrogel systems as a possible mechanism for alterations in gel properties using both SDS–PAGE and proteomic analysis via LC–MS/MS. Furthermore, this is the first time any hydrogel derived from decellularized dermis has been characterized with proteomics.[10] In addition, this work demonstrates that the tunability of these gels has physiological implications, because we observe tunability in cell migration through the gel in vitro and cell invasion in vivo.

Hydrogels have long been investigated in the context of compromised wound healing because they can maintain a hydrated environment and manipulate cell interactions and invasion after injury.[46,47] Furthermore, they can be loaded with cells or drugs to deliver therapeutics locally to the wound environment.[5,46,48–50] Most hydrogels used for wound care in the clinic function simply to keep the wound hydrated and/or to absorb any wound exudate, with the notable exception of Apligraf, a collagen hydrogel containing live human fibro-blasts.[51–53] Recently, biological materials and tissue-derived hydrogels have generated interest as wound treatments, because they retain the complexity and bioactivity of the native ECM and can be readily implemented in the clinic.[52] A hydrogel composed of adipose-derived ECM and methylcellulose accelerated re-epithelialization in rats, an effect that was amplified by the inclusion of stem cells within the gel.[54] Another study found that dermis-derived hydrogels trended toward improved healing in rats, although the study found no statistically significant changes.[55] A combination of a growing body of literature and tremendous clinical need led us to test our hydrogels in a compromised wound healing setting. When applied to chronic diabetic wounds in a mouse, TSP-2 KO hydrogels enhanced vascularization and remodeling over WT. Additionally, TSP-2 KO gels promoted greater epithelialization compared to WT gels or no treatment at 10 days, and KO gels significantly enhanced overall wound repair compared to no treatment at 21 days. Overall, TSP-2 KO hydrogels accelerated wound healing in diabetic animals without the addition of exogenous growth factors or cells. This is consistent with previous findings that intact TSP-2 null decellularized skin or CDM enables increased endothelial cell and fibroblast migration through the material and that breakdown products of TSP-2 null decellularized skin have favorable chemotactic properties.[25,56]

Finally, we have demonstrated that it is possible to construct hydrogels from CDM and that, when the source cells are genetically manipulated, tunable mechanical properties are achievable with similar trends to those observed for tissue-derived hydrogels. It is of note that the overall storage moduli are much lower from hydrogels prepared with decellularized tissues. This suggests that rapid genetic engineering and screening of ECM-derived hydrogels could accelerate discovery of other hydrogels with novel properties. Additionally, this technique could also be performed with human or porcine cells to create genetically engineered matrix materials suitable for clinical translation. However,

the lower storage moduli will likely need to be overcome via optimizing ECM production, solubilization, and concentration for this new system. Ultimately, this work provides a foundation for using genetically engineered ECM to create tunable in vitro culture systems and pro-regenerative materials for clinical use.

CONCLUSIONS

We have developed genetically tunable ECM-derived materials by forming hydrogels from tissues and CDM derived from both WT and TSP-2 KO sources. In general, TSP-2 KO hydrogels exhibited reduced storage moduli and increased cell invasion compared to WT (in vitro and in vivo), with the 1:1 mixture having intermediate properties. Furthermore, TSP-2 KO hydrogels promoted enhanced wound healing in a compromised diabetic wound healing model, with increased vascularization, epithelialization, gel remodeling, and a reduction in the overall size of the wound bed, highlighting the regenerative potential of genetically tunable ECM-derived materials. Finally, we demonstrated feasibility to form tunable gels from CDM, a system that can be harnessed to rapidly screen genetic alterations, or harness human or porcine cells to create materials for the clinic.

Supplementary Material

Refer to Web version on PubMed Central for supplementary material.

ACKNOWLEDGMENTS

We would like to thank Gilad Kaufman and Chinedum Osuji for helpful advice and the use of their rheometer. This work was funded by the National Institutes of Health (grant GM-072194). This material is based upon work supported by the National Science Foundation Graduate Research Fellowship under Grant No. DGE-1122492 (A.H.M.). Any opinion, findings, and conclusions or recommendations expressed in this material are those of the authors and do not necessarily reflect the views of the National Science Foundation. Use of core facilities was supported by YINQE and NSF MRSEC DMR 1119826. We would also like to thank Yale School of Medicine for funding the Q Exactive Plus LC-MS/MS system located within the Yale Mass Spectrometry (MS) & Proteomics Resource of the W.M. Keck Foundation Biotechnology Resource Laboratory and Jean Kanyo, Edward Voss, and TuKiet Lam for helping with MS sample preparation, data collection, and analysis.

REFERENCES

(1). Londono R; Badylak SF Biologic Scaffolds for Regenerative Medicine: Mechanisms of In Vivo Remodeling. Ann. Biomed. Eng 2015, 43, 577–592. [PubMed: 25213186]

(2). Tian R; Qiu X; Yuan P; Lei K; Wang L; Bai Y; Liu S; Chen X Fabrication of Self-Healing Hydrogels with On-Demand Antimicrobial Activity and Sustained Biomolecule Release for Infected Skin Regeneration. ACS Appl. Mater. Interfaces 2018, 10, 17018–17027. [PubMed: 29693373]

(3). Han WM; Jang YC; García AJ Engineered Matrices for Skeletal Muscle Satellite Cell Engraftment and Function. Matrix Biol. 2017, 60–61, 96–109.

(4). Morris AH; Stamer DK; Kyriakides TR The Host Response to Naturally-Derived Extracellular Matrix Biomaterials. Semin. Immunol 2017, 29, 72–91. [PubMed: 28274693]

(5). Dimatteo R; Darling NJ; Segura T In Situ Forming Injectable Hydrogels for Drug Delivery and Wound Repair. Adv. Drug Deliv. Rev 2018, 127, 167–184. [PubMed: 29567395]

(6). Aamodt JM; Grainger DW Extracellular Matrix-Based Biomaterial Scaffolds and the Host Response. Biomaterials 2016, 86, 68–82. [PubMed: 26890039]

(7). Morris AH; Kyriakides TR Matricellular Proteins and Biomaterials. Matrix Biol. 2014, 37, 183–191. [PubMed: 24657843]

(8). Damania A; Kumar A; Teotia AK; Kimura H; Kamihira M; Ijima H; Sarin SK; Kumar A Decellularized Liver Matrix-Modified Cryogel Scaffolds as Potential Hepatocyte Carriers in Bioartificial Liver Support Systems and Implantable Liver Constructs. ACS Appl. Mater. Interfaces 2017, 10, 114–126. [PubMed: 29210278]

(9). Sawkins MJ; Saldin LT; Badylak SF; White LJ ECM Hydrogels for Regenerative Medicine. In Extracellular Matrix for Tissue Engineering and Biomaterials; Berardi AC, Ed.; Springer International Publishing: Cham, Switzerland, 2018; pp 27–58.

(10). Saldin LT; Cramer MC; Velankar SS; White LJ; Badylak SF Extracellular Matrix Hydrogels from Decellularized Tissues: Structure and Function. Acta Biomater. 2017, 49, 1–15. [PubMed: 27915024]

(11). Slivka PF; Dearth CL; Keane TJ; Meng FW; Medberry CJ; Riggio RT; Reing JE; Badylak SF Fractionation of an ECM Hydrogel into Structural and Soluble Components Reveals Distinctive Roles in Regulating Macrophage Behavior. Biomater. Sci 2014, 2, 1521. [PubMed: 26829566]

(12). Wang W; Zhang X; Chao NN; Qin TW; Ding W; Zhang Y; Sang JW; Luo JC Preparation and Characterization of Pro-Angiogenic Gel Derived from Small Intestinal Submucosa. Acta Biomater. 2016, 29, 135–148. [PubMed: 26472613]

(13). Agrawal V; Tottey S; Johnson SA; Freund JM; Siu BF; Badylak SF Recruitment of Progenitor Cells by an Extracellular Matrix Cryptic Peptide in a Mouse Model of Digit Amputation. Tissue Eng. Part A 2011, 17, 2435–2443. [PubMed: 21563860]

(14). Beattie AJ; Gilbert TW; Guyot JP; Yates AJ; Badylak SF Chemoattraction of Progenitor Cells by Remodeling Extracellular Matrix Scaffolds. Tissue Eng. Part A 2009, 15, 1119–1125. [PubMed: 18837648]

(15). Seif-Naraghi SB; Singelyn JM; Salvatore MA; Osborn KG; Wang JJ; Sampat U; Kwan OL; Strachan GM; Wong J; Schup-Magoffin PJ; et al. Safety and Efficacy of an Injectable Extracellular Matrix Hydrogel for Treating Myocardial Infarction. Sci. Transl. Med 2013, 5, 173ra25.

(16). Rao N; Agmon G; Tierney MT; Ungerleider JL; Braden RL; Sacco A; Christman KL Engineering an Injectable Muscle-Specific Microenvironment for Improved Cell Delivery Using a Nanofibrous Extracellular Matrix Hydrogel. ACS Nano 2017, 11, 3851–3859. [PubMed: 28323411]

(17). Yuan X; Wei Y; Villasante A; Ng JJD; Arkonac DE; Chao PG; Vunjak-Novakovic G Stem Cell Delivery in Tissue-Specific Hydrogel Enabled Meniscal Repair in an Orthotopic Rat Model. Biomaterials 2017, 132, 59–71. [PubMed: 28407495]

(18). Romero-López M; Trinh AL; Sobrino A; Hatch MMS; Keating MT; Fimbres C; Lewis DE; Gershon PD; Botvinick EL; Digman M; et al. Recapitulating the Human Tumor Microenvironment: Colon Tumor-Derived Extracellular Matrix Promotes Angiogenesis and Tumor Cell Growth. Biomaterials 2017, 116, 118–129. [PubMed: 27914984]

(19). Sonnenberg SB; Rane AA; Liu CJ; Rao N; Agmon G; Suarez S; Wang R; Munoz A; Bajaj V; Zhang S; et al. Delivery of an Engineered HGF Fragment in an Extracellular Matrix- Derived Hydrogel Prevents Negative LV Remodeling Post-Myocardial Infarction. Biomaterials 2015, 45, 56–63. [PubMed: 25662495]

(20). Seif-Naraghi SB; Horn D; Schup-Magoffin PJ; Christman KL Injectable Extracellular Matrix Derived Hydrogel Provides a Platform for Enhanced Retention and Delivery of a Heparin-Binding Growth Factor. Acta Biomater. 2012, 8, 3695–3703. [PubMed: 22750737]

(21). Wolf MT; Daly KA; Brennan-Pierce EP; Johnson SA; Carruthers CA; D'Amore A; Nagarkar SP; Velankar SS; Badylak SF A Hydrogel Derived from Decellularized Dermal Extracellular Matrix. Biomaterials 2012, 33, 7028–7038. [PubMed: 22789723]

(22). Freytes DO; Martin J; Velankar SS; Lee AS; Badylak SF Preparation and Rheological Characterization of a Gel Form of the Porcine Urinary Bladder Matrix. Biomaterials 2008, 29, 1630–1637. [PubMed: 18201760]

(23). Medberry CJ; Crapo PM; Siu BF; Carruthers CA; Wolf MT; Nagarkar SP; Agrawal V; Jones KE; Kelly J; Johnson SA; et al. Hydrogels Derived from Central Nervous System Extracellular Matrix. Biomaterials 2013, 34, 1033–1040. [PubMed: 23158935]

(24). Ghuman H; Massensini AR; Donnelly J; Kim S-M; Medberry CJ; Badylak SF; Modo M ECM Hydrogel for the Treatment of Stroke: Characterization of the Host Cell Infiltrate. Biomaterials 2016, DOI: 10.1016/j.biomaterials.2016.03.014.

(25). Morris AH; Stamer DK; Kunkemoeller B; Chang J; Xing H; Kyriakides TR Decellularized Materials Derived from TSP2-KO Mice Promote Enhanced Neovascularization and Integration in Diabetic Wounds. Biomaterials 2018, 169, 61–71. [PubMed: 29631168]

(26). Bourgine PE; Gaudiello E; Pippenger B; Jaquiery C; Klein T; Pigeot S; Todorov A Jr.; Feliciano S; Banfi A; Martin I Engineered Extracellular Matrices as Biomaterials of Tunable Composition and Function. Adv. Funct. Mater 2017, 27, 1605486.

(27). Kristofik NJ; Qin L; Calabro NE; Dimitrievska S; Li G; Tellides G; Niklason LE; Kyriakides TR Improving in Vivo Outcomes of Decellularized Vascular Grafts via Incorporation of a Novel Extracellular Matrix. Biomaterials 2017, 141, 63–73. [PubMed: 28667900]

(28). Kristofik N; Calabro NE; Tian W; Meng A; MacLauchlan S; Wang Y; Breuer CK; Tellides G; Niklason LE; Kyriakides TR Impaired von Willebrand Factor Adhesion and Platelet Response in Thrombospondin-2 Knockout Mice. Blood 2016, 128, 1642–1650. [PubMed: 27471233]

(29). Morris AH; Chang J; Kyriakides TR Inadequate Processing of Decellularized Dermal Matrix Reduces Cell Viability In Vitro and Increases Apoptosis and Acute Inflammation In Vivo. Biores. Open Access 2016, 5, 177–187. [PubMed: 27500014]

(30). Reing JE; Zhang L; Myers-Irvin J; Cordero KE; Freytes DO; Heber-Katz E; Bedelbaeva K; McIntosh D; Dewilde A; Braunhut SJ; Badylak SF Degradation Products of Extracellular Matrix Affect Cell Migration and Proliferation. Tissue Eng. Part A 2009, 15, 605–614. [PubMed: 18652541]

(31). Addison WN; McKee MD Inositol Hexakisphosphate Inhibits Mineralization of MC3T3-E1 Osteoblast Cultures. Bone 2010, 46, 1100–1107. [PubMed: 20079473]

(32). Kyriakides TR; Tam JWY; Bornstein P Accelerated Wound Healing in Mice With a Disruption of the Thrombospondin 2 Gene. J. Invest. Dermatol 1999, 113, 782–787. [PubMed: 10571734]

(33). Kobsa S; Kristofik NJ; Sawyer AJ; Bothwell ALM; Kyriakides TR; Saltzman WM An Electrospun Scaffold Integrating Nucleic Acid Delivery for Treatment of Full-Thickness Wounds. Biomaterials 2013, 34, 3891–3901. [PubMed: 23453058]

(34). Klein ZA; Takahashi H; Ma M; Stagi M; Zhou M; Lam TKT; Strittmatter SM Loss of TMEM106B Ameliorates Lysosomal and Frontotemporal Dementia-Related Phenotypes in Progranulin-Deficient Mice. Neuron 2017, 95, 281–296.e6. [PubMed: 28728022]

(35). Fitzpatrick LE; McDevitt TC Cell-Derived Matrices for Tissue Engineering and Regenerative Medicine Applications. Biomater. Sci 2015, 3, 12–24. [PubMed: 25530850]

(36). Bancroft T; Bouaouina M; Roberts S; Lee M; Calderwood DA; Schwartz M; Simons M; Sessa WC; Kyriakides TR Up-Regulation of Thrombospondin-2 in Akt1-Null Mice Contributes to Compromised Tissue Repair Due to Abnormalities in Fibroblast Function. J. Biol. Chem 2015, 290, 409–422. [PubMed: 25389299]

(37). Bergmeister H; Boeck P; Kasimir M-T; Fleck T; Fitzal F; Husinsky W; Mittlboeck M; Stoehr HG; Losert U; Wolner E; Grabenwoeger M Effect of Laser Perforation on the Remodeling of Acellular Matrix Grafts. J. Biomed. Mater. Res., Part B Appl. Biomater 2005, 74B, 495–503.

(38). Kasyanov VA; Hodde J; Hiles MC; Eisenberg C; Eisenberg L; De Castro LEF; Ozolanta I; Murovska M; Draughn RA; Prestwich GD; et al. Rapid Biofabrication of Tubular Tissue Constructs by Centrifugal Casting in a Decellularized Natural Scaffold with Laser-Machined Micropores. J. Mater. Sci. Mater. Med 2009, 20, 329–337. [PubMed: 18807150]

(39). Sheridan WS; Duffy GP; Murphy BP Mechanical Characterization of a Customized Decellularized Scaffold for Vascular Tissue Engineering. J. Mech. Behav. Biomed. Mater 2012, 8, 58–70. [PubMed: 22402154]

(40). Evren S; Loai Y; Antoon R; Islam S; Yeger H; Moore K; Wong K; Gorczynski R; Farhat WA Urinary Bladder Tissue Engineering Using Natural Scaffolds in a Porcine Model: Role of Toll-like Receptors and Impact of Biomimetic Molecules. Cells Tissues Organs 2010, 192, 250–261. [PubMed: 20588005]

(41). De Cock LJ; De Koker S; De Vos F; Vervaet C; Remon JP; De Geest BG Layer-by-Layer Incorporation of Growth Factors in Decellularized Aortic Heart Valve Leaflets. Biomacromolecules 2010, 11, 1002–1008. [PubMed: 20155947]

(42). Koobatian MT; Row S; Smith RJ Jr.; Koenigsknecht C; Andreadis ST; Swartz DD Successful Endothelialization and Remodeling of a Cell-Free Small-Diameter Arterial Graft in a Large Animal Model. Biomaterials 2016, 76, 344–358. [PubMed: 26561932]

(43). D'Amore A; Yoshizumi T; Luketich SK; Wolf MT; Gu X; Cammarata M; Hoff R; Badylak SF; Wagner WR Bi-Layered Polyurethane – Extracellular Matrix Cardiac Patch Improves Ischemic Ventricular Wall Remodeling in a Rat Model. Biomaterials 2016, 107, 1–14. [PubMed: 27579776]

(44). Gothard D; Smith EL; Kanczler JM; Black CR; Wells JA; Roberts CA; White LJ; Qutachi O; Peto H; Rashidi H; et al. In Vivo Assessment of Bone Regeneration in Alginate/Bone ECM Hydrogels with Incorporated Skeletal Stem Cells and Single Growth Factors. PLoS One 2015, 10, e0145080. [PubMed: 26675008]

(45). Bracaglia LG; Fisher JP Extracellular Matrix-Based Biohybrid Materials for Engineering Compliant, Matrix-Dense Tissues. Adv. Healthc. Mater 2015, 4, 2475–2487. [PubMed: 26227679]

(46). Hubbell JA Hydrogel Systems for Barriers and Local Drug Delivery in the Control of Wound Healing. J. Controlled Release 1996, 39, 305–313.

(47). Kirker KR; Luo Y; Nielson JH; Shelby J; Prestwich GD Glycosaminoglycan Hydrogel Films as Bio-Interactive Dressings for Wound Healing. Biomaterials 2002, 23, 3661–3671. [PubMed: 12109692]

(48). Sun G; Zhang X; Shen Y-I; Sebastian R; Dickinson LE; Fox-Talbot K; Reinblatt M; Steenbergen C; Harmon JW; Gerecht S Dextran Hydrogel Scaffolds Enhance Angiogenic Responses and Promote Complete Skin Regeneration during Burn Wound Healing. Proc. Natl. Acad. Sci 2011, 108, 20976–20981. [PubMed: 22171002]

(49). Obara K; Ishihara M; Ishizuka T; Fujita M; Ozeki Y; Maehara T; Saito Y; Yura H; Matsui T; Hattori H; et al. Photocrosslinkable Chitosan Hydrogel Containing Fibroblast Growth Factor-2 Stimulates Wound Healing in Healing-Impaired Db/Db Mice. Biomaterials 2003, 24, 3437–3444. [PubMed: 12809772]

(50). Dash B; Xu Z; Lin L; Koo A; Ndon S; Berthiaume F; Dardik A; Hsia H Stem Cells and Engineered Scaffolds for Regenerative Wound Healing. Bioengineering 2018, 5, 23. [PubMed: 29522497]

(51). Dickinson LE; Gerecht S Engineered Biopolymeric Scaffolds for Chronic Wound Healing. Front. Physiol 2016, 7, 341. [PubMed: 27547189]

(52). Turner NJ; Badylak SF The Use of Biologic Scaffolds in the Treatment of Chronic Nonhealing Wounds. Adv. Wound Care 2015, 4, 490–500.

(53). Kamoun EA; Kenawy ERS; Chen X A Review on Polymeric Hydrogel Membranes for Wound Dressing Applications: PVA-Based Hydrogel Dressings. J. Adv. Res 2017, 8, 217–233. [PubMed: 28239493]

(54). Kim EJ; Choi JS; Kim JS; Choi YC; Cho YW Injectable and Thermosensitive Soluble Extracellular Matrix and Methylcellulose Hydrogels for Stem Cell Delivery in Skin Wounds. Biomacromolecules 2015, 17, 4–11. [PubMed: 26607961]

(55). Engel H; Kao S-W; Larson J; Uriel S; Jiang B; Brey EM; Cheng M-H Investigation of Dermis-derived Hydrogels for Wound Healing Applications. Biomed. J 2015, 38, 58–64. [PubMed: 25179708]

(56). Krady MM; Zeng J; Yu J; MacLauchlan S; Skokos EA; Tian W; Bornstein P; Sessa WC; Kyriakides TR Thrombospondin-2 Modulates Extracellular Matrix Remodeling during Physiological Angiogenesis. Am. J. Pathol 2008, 173, 879–891. [PubMed: 18688033]

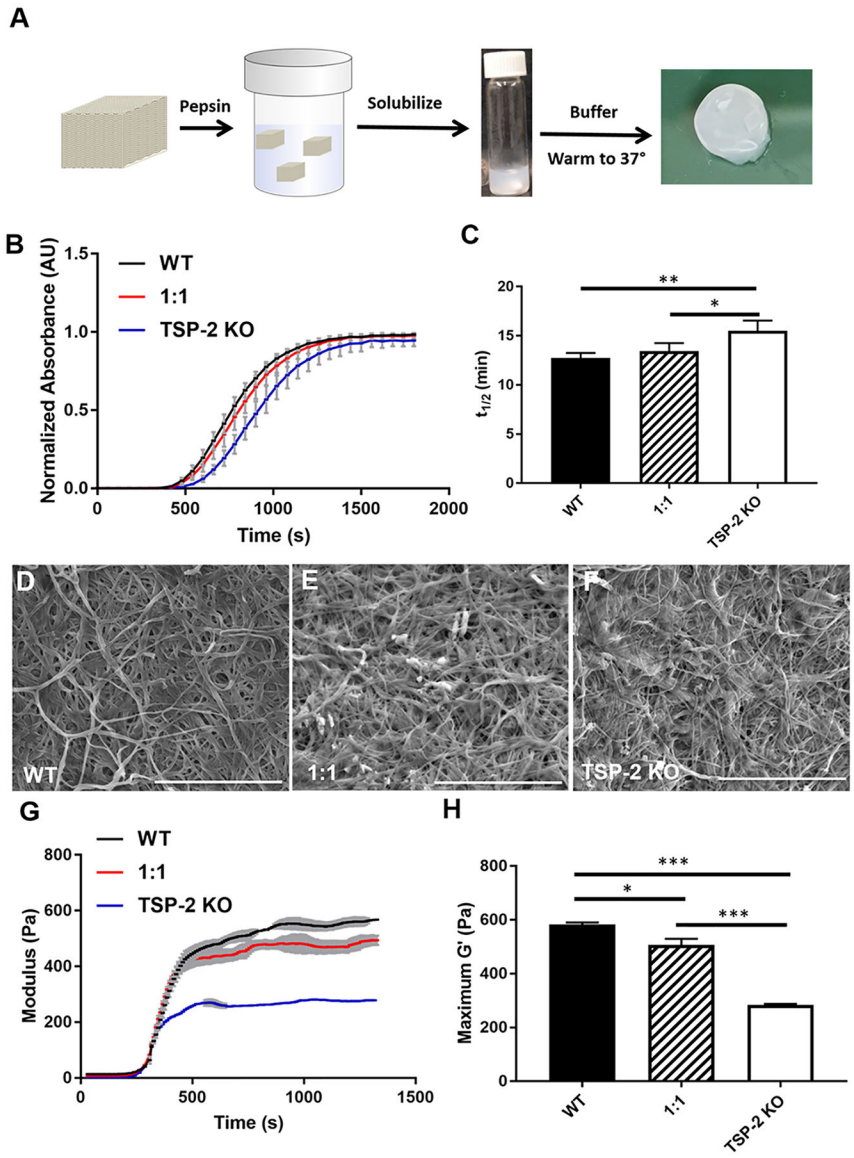

Figure 1.

Genetic manipulation permits tunability of tissue-derived hydrogels. (A) Schematic of hydrogel preparation and example macroscopic image of hydrogel. (B) Optical density during gelation and (C) the time to half gelation of 4 mg/mL hydrogels ($n = 5$). (D–F) Representative SEM images of (D) WT, (E) 1:1, and (F) TSP-2 KO gel show similar structures. Scale bars = 5 μm. (G) Rheology reveals overall changes in maxima and suggests tunability of mechanical properties between WT, TSP-2 KO, and a 1:1 mixture (rheological traces are given as mean ± SEM). (H) Analysis of rheological data indicates significant changes between maximum storage moduli with genotype of matrix ($n = 3$). Results are given as mean + SEM, *$p < 0.05$, **$p < 0.01$, ***$p < 0.005$.

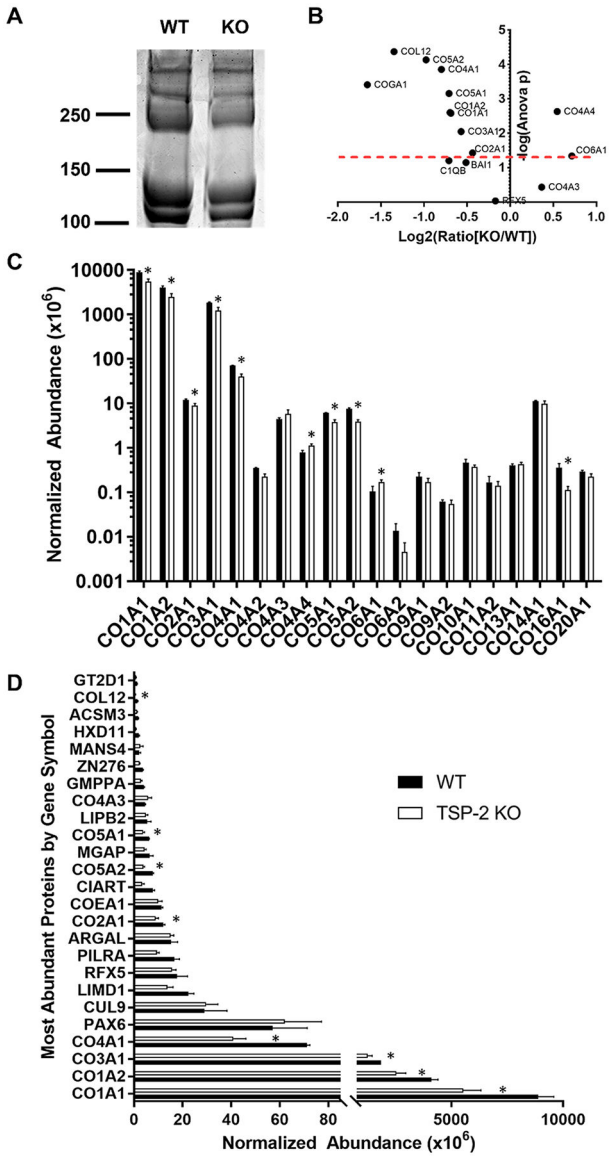

Figure 2.

Proteomics reveals subtle changes in composition of hydrogels between genotypes. (A) SDS–PAGE demonstrates qualitative differences in the protein content of WT and TSP-2 KO gels. (B) A volcano plot of quantitative proteomics results demonstrates significant differences between WT and TSP-2 KO (above the red dashed line is $p < 0.05$). (C) Collagen abundance from quantitative proteomics exhibits similar, albeit altered, levels between genotypes. (D) The top 25 most abundant proteins show differences between WT and TSP-2 KO gels. Results are given as mean + SEM, $n = 3$, $^*p < 0.05$.

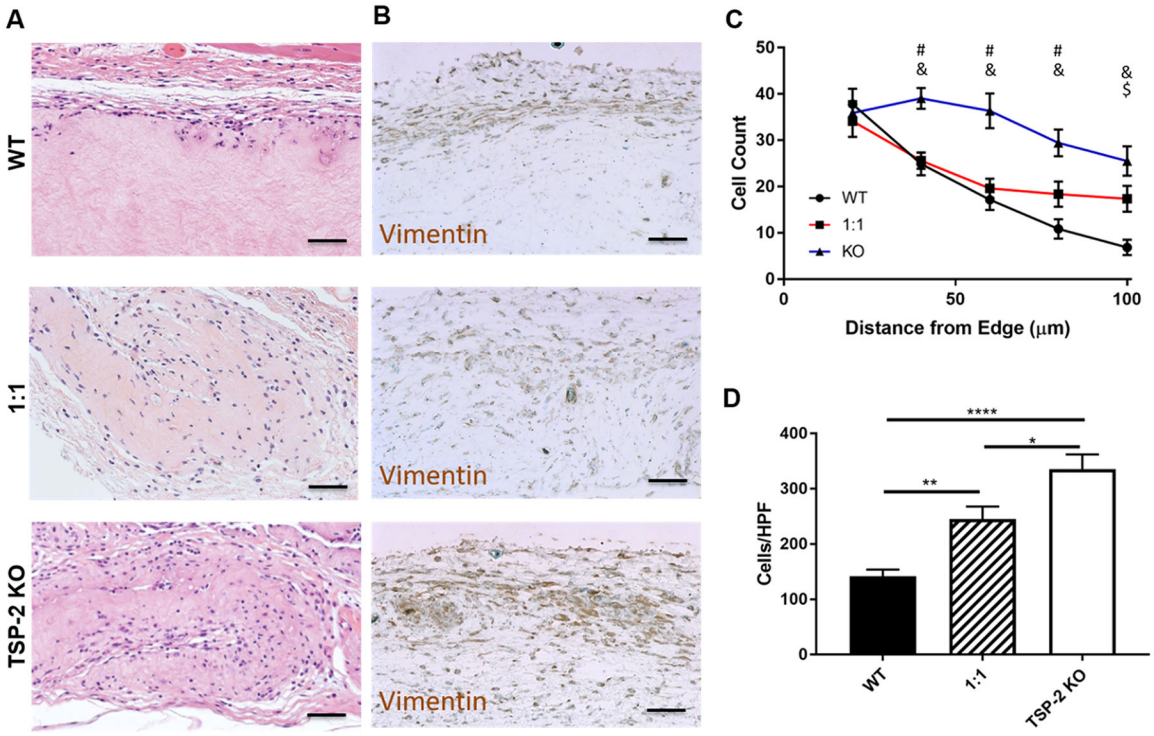

Figure 3.

Genetic manipulation permits tunability of cell invasion into tissue-derived hydrogels. (A) Representative H&E images indicate higher cell presence in TSP-2 KO gels that were implanted subcutaneously in healthy mice for 5 days. (B) Vimentin staining indicates that many of the cells present were of mesenchymal lineage. (C) Quantification shows that cells penetrated further into TSP-2 KO hydrogels and (D) an increasing ratio of TSP-2 KO matrix in the hydrogel resulted in increased total cellular content. Scale bars = 50 μm. Results are given as mean + SEM [±SEM for (C)], $n = 8$, *$p < 0.05$, **$p < 0.01$, ****$p < 0.001$. # indicates that TSP-2 KO is different from WT, $ indicates that 1:1 is different from WT, and & indicates that 1:1 is different from TSP-2 KO, $p < 0.05$.

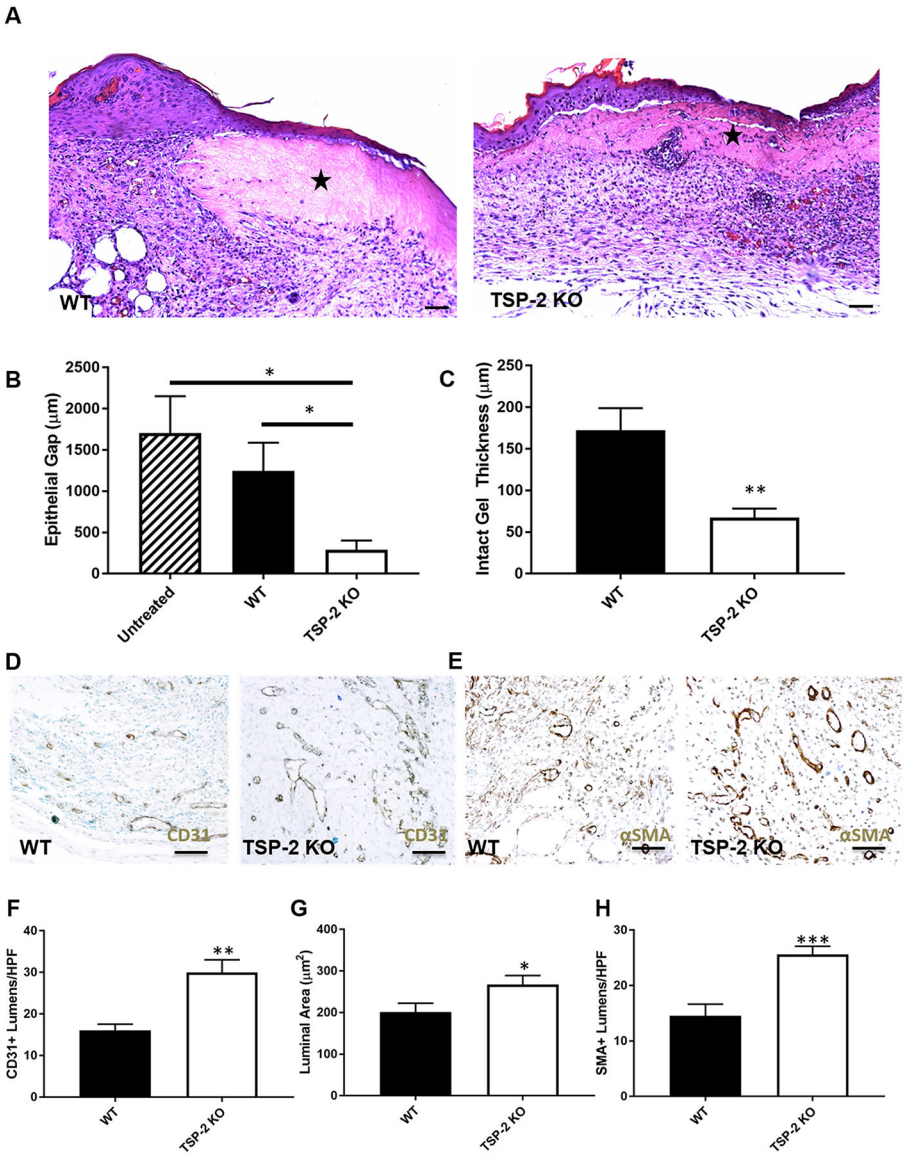

Figure 4.

Improved diabetic wound closure and vascularization with TSP-2 KO hydrogels in mice. (A) Representative images of H&E staining indicate higher cell presence within TSP-2 KO gels that were implanted into full-thickness diabetic wounds for 10 days. (B) TSP-2 KO gel demonstrates a decreased epithelial gap at 10 days. (C) Additionally, the thickness of the remaining gel is reduced with TSP-2 KO gel, suggesting increased remodeling. (D, E) Representative images of (D) CD31 stains and (E) αSMA stains. (F–H) Quantification of CD31 and αSMA stains reveals increased (F) vessel density, (G) size, and (H) maturity in wound beds treated with TSP-2 KO gel. Scale bars = 50 μm. Results are given as mean + SEM, $n = 4$ (untreated), $n = 9$ (gel-treated), $^{*}p < 0.05$, $^{**}p < 0.01$.

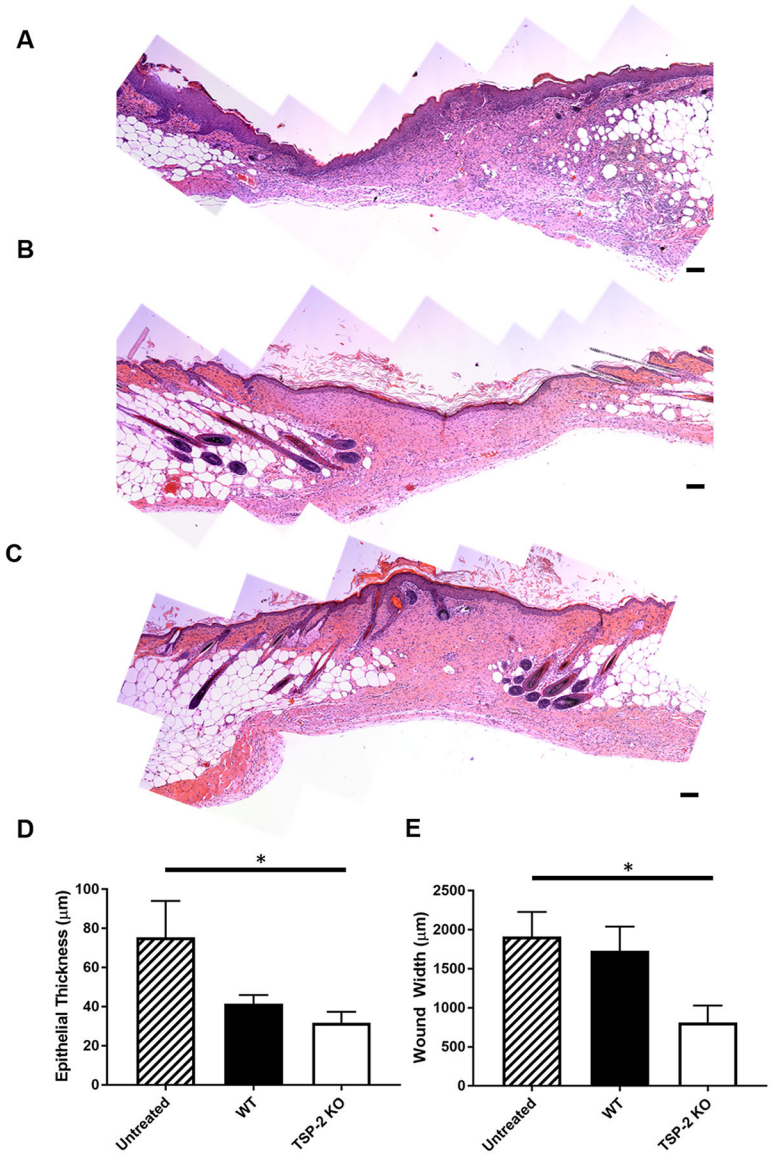

Figure 5.

TSP-2 KO hydrogels improved diabetic wound resolution compared to untreated wounds in mice. (A–C) Representative stitched images of entire wound beds from diabetic mice after 21 days of healing that were (A) untreated, (B) WT gel-treated, or (C) TSP-2 KO gel-treated. (D) TSP-2 KO-treated wounds demonstrate decreased epithelial thickness (a measure of maturity) by 21 days when compared to untreated control. (E) TSP-2 KO gel demonstrates decreased wound width at 21 days. Scale bars = 100 μm. Results are given as mean + SEM, $n = 5$ (untreated and WT gel-treated), $n = 6$ (KO gel-treated), $^*p < 0.05$.

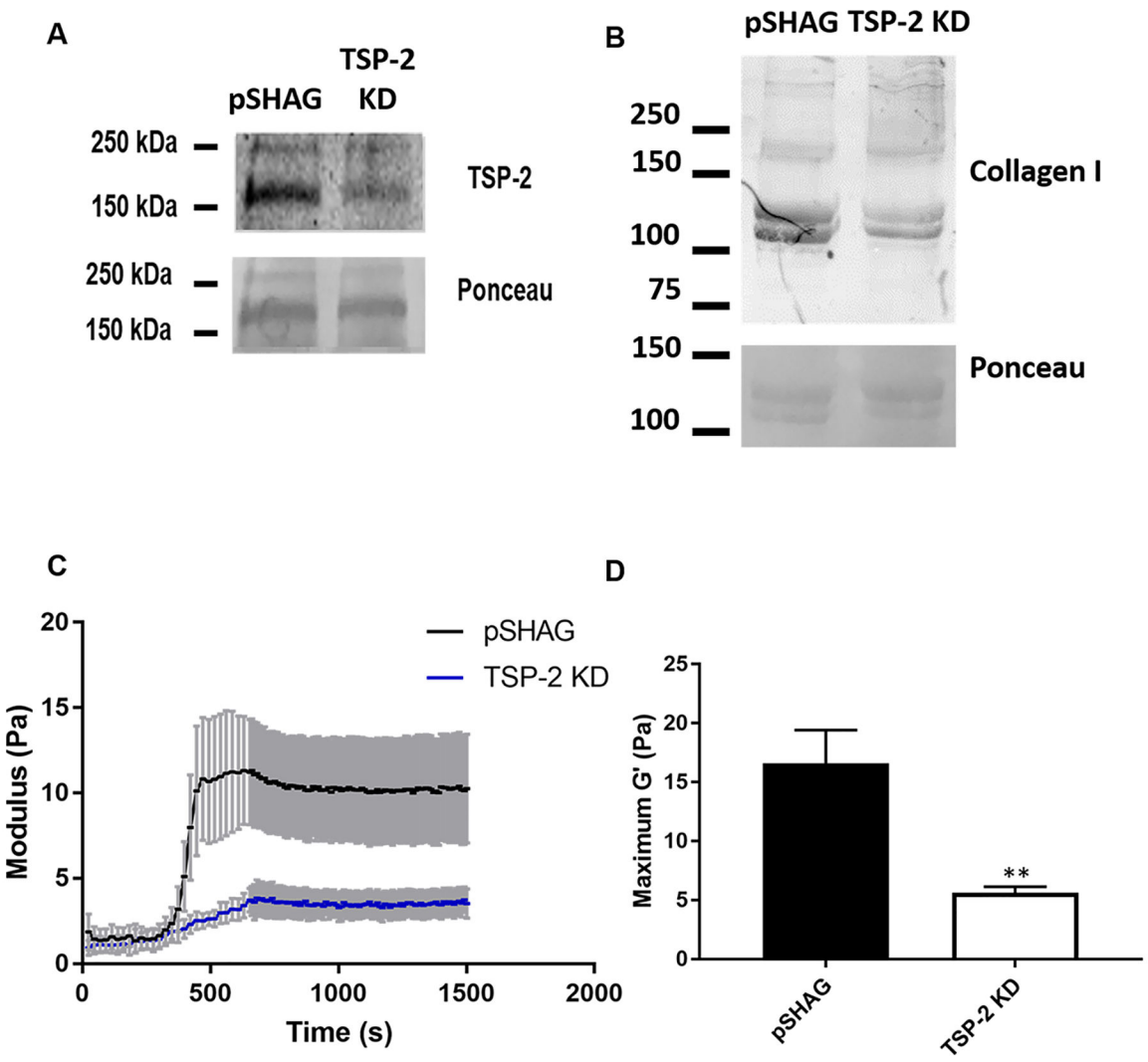

Figure 6.

Hydrogels prepared from CDM exhibit similar trends to tissue-derived hydrogels. (A) Western blot reveals successful reduction of TSP-2 expression in MC3T3-E1 cells via transfection of an shRNA. (B) Western blot of pre-gel solution demonstrates that the TSP-2 KD gels exhibit a reduction in the expression of collagen type I. (C, D) Rheology shows that hydrogels prepared from MC3T3-E1 CDM exhibit similar trends to tissue-derived hydrogels, (C) with the vector control exhibiting a higher modulus than TSP-2 KD (n = 6) (rheological traces are given as mean ± SEM), with (D) quantification of the maximal storage modulus demonstrating a significant reduction in the TSP-2 KD samples. Results are given as mean + SEM, (n = 6), **p < 0.01.